International Journal of Advanced Engineering, Management and Science (IJAEMS)
Peer-Reviewed Journal
ISSN: 2454-1311 | Vol-11, Issue-4; Jul-Aug, 2025
Journal Home Page: https://ijaems.com/
DOI: https://dx.doi.org/10.22161/ijaems.114.7

Investigating the Effects of Geogrid Aperture Shapes on Load-Deformation Behavior and Crack Propagation in Plain Concrete Footings

E. A. El-Kasaby [1], Mahmoud Awwad [2], Mohab. R. El-Ashmony [3], A. A. Abo-Shark [4]

[1] Prof. of soil mechanics and foundations, Civil Engineering Department, Benha Faculty of Engineering, Benha University, Cairo, Egypt.
[2, 3 4]Lecturer, Civil Engineering Department, Benha Faculty of Engineering, Benha University, Cairo, Egypt.

Received: 02 Jun 2025; Received in revised form: 30 Jun 2025; Accepted: 04 Jul 2025; Available online: 09 Jul 2025

Abstract *— Geogrid reinforcement is a widely used technique for improving the mechanical properties of infrastructure engineering structures. However, there is limited understanding of the behavior of geogrid with different aperture shapes when used as reinforcement in plain concrete footings. This paper presents a comprehensive study that investigates the effects of five different aperture shapes of geogrid reinforcement on the load-deformation behavior and crack propagation of plain concrete footings. The study also aims to provide a basis for future research on the use of geogrid as reinforcement in thin concrete overlays. The five geogrid products used in this study were characterized based on their index material properties, and were used in combination with fiber glass reinforced concrete (FGRC) and normal concrete mixes. The experiments were conducted on both unreinforced footings and footings reinforced with one layer of geogrid. A distributed static load was applied to simulate the stress of reinforced footings. The experimental results indicate that the strength resistance of the geogrid reinforced footings is significantly improved compared to the unreinforced footings. The use of glass fibers and geogrid confinement in the footing designs were found to have a significant impact on improving the load-deformation behavior and crack propagation. Furthermore, the study reveals that the strength and dimensions of the geogrid reinforcement play a crucial role in determining the behavior of the plain concrete footings. Also, the Comparison between cast and load capacity of all samples was presented.*

Keywords *— **Geosynthetics, Fiber glass, plain concrete footing, shallow foundations, triaxial geogrid, biaxial geogrid, FGRC.***

I. INTRODUCTION

Geo-grid is one of the geo-synthetic constituent materials; it is made up of polymers such as polyethylene, polypropylene, and polyester. These geo-grids can be classified into uniaxial, bi-axial, and tri-axial categories. Uni-axial geo-grids are mainly used for grade separation applications, such as retaining walls and precipitous slopes, and bi-axial and tri-axial geo-grids are primarily used for roadway applications. Several studies have investigated the effective use of geo-grid as a reinforcing material with plain cement concrete in thin sections where steel reinforcement is not possible [1][2].

Recent research has investigated the use of geogrid in concrete construction. It was effective and less difficult in a corrosive environment due to Geo-Grid's usability. Geo-grid confinement is an alternative solution for tensile reinforcement [3, 4]. For the

efficient transfer of tensile tension and the enhancement of the composite action of steel fiber-reinforced concrete, the fiber-using geo-grid is the better option [5]. However, without any practical difficulty, these geogrid reinforcing materials will improve the bonding behavior of concrete. The geogrid could increase the bending and compressive strengths of concrete, as well as the resistance to crack propagation in specimens confined by one, two, or three layers of geogrid. [6]. In addition, many researchers studied the behavior of prismatic and cylindrical specimens confined between one and two geogrid layers [7][8].

Glass fiber-reinforced concrete (GFRC) material is being used in recent innovations to increase the strength of the concrete [9]. This glass fiber will have great strength in concrete. These fibers are composite materials consisting of a matrix with an asymmetrical dispersion or distribution of minute natural or synthetic fibers. [10]. The shear-friction strength of concrete will be increased, and this isolated fiber will also serve as an effective shear reinforcement. The crack propagation in the beam will effectively be reduced by using glass fibers [11]. From the applied load, the beam will carry tensile stresses with the presence of arbitrarily dispersed glass fibers. Consequently, the tensile strength of the concrete in GFRC will be improved. In addition to preventing fracture propagation, these fibers also bridge tensile cracks [12].Shakor and Pimplikar [13] studied the trail tests for concrete with glass fiber and without glass fiber are conducted to indicate the differences in compressive strength and flexural strength by using cubes of varying sizes. Ibrahim [14] comparing the results of GFRC with plain concrete and validated the positive effect of glass fibers with percentage increase in compression, splitting and flexure improvement of specimens.

Geogrid with glass fiber may be a better choice for effective transfer of tensile stress and to enhance the concrete section. These strengthening materials may also impart better bonding behavior with concrete without practical difficulty. In the present study, the effect of geogrid with glass fibers on plain concrete footing has been investigated. Under a distributed static load, twelve footing specimens have been tested. In order to examine the effect of glass fibers and geogrid reinforcement, the load–deflection and rigidity degradation with failure patterns of various specimens are compared with those of conventional specimens. This study could identify new options and pave the way for the introduction of geogrid into structural concrete sections. The main goal of this study is to investigate the behavior of biaxial geogrid or triaxial geogrid with glass fibers and to determine the experimental effect of using these combinations in footing specimens.

II. EXPERIMENTAL PROGEAM

The study involved experimentation on a set of twelve square plain concert footings specimens made of plain concrete mixture. The specimens, with dimensions and loading details as depicted in Figure 1, were 30 cm in length and 5 cm in thickness. The footings were segregated into six categories, comprising one unreinforced plain specimen designated as control 1, one fiber reinforced plain specimen referred to as control 2, three specimens reinforced with one layer of tri-axial geogrid, two specimens fortified with one layer of biaxial geogrid, three specimens fortified with one layer of tri-axial geogrid using GFRC, and two specimens reinforced with one layer of biaxial geogrid using GFRC. Table1, summarizes all of the various configurations of the footing specimens that were tested.

Table 1: Comprehensive Configuration Details of Footing Specimens

Group Name	Reinforced Material	Code of Specimen	Descreptions
Control 1	-	**P1**	**Plain Concrete**
Triaxial	Tx 130	P2	Concrete with Triaxial geogrid Tx130
	Tx 150	P3	Concrete with Triaxial geogrid Tx150
	Tx 160	P4	Concrete with Triaxial geogrid Tx160
Biaxial	SS30	P5	Concrete with biaxial geogrid SS30

	SS40	P6	Concrete with biaxial geogrid SS40
Control 2	-	**P7**	**GFRC - 900gm/m³**
Triaxial with glass fiber	F-Tx 130	P8	GFRC and Tri axial geogrid Tx130
	F-Tx 150	P9	GFRC and Triaxial geogrid Tx150
	F-Tx 160	P10	GFRC and Triaxial geogrid Tx160
Biaxial with glass fiber	F-SS30	P11	GFRC and biaxial geogrid SS30
	F-SS40	P12	GFRC and biaxial geogrid SS40

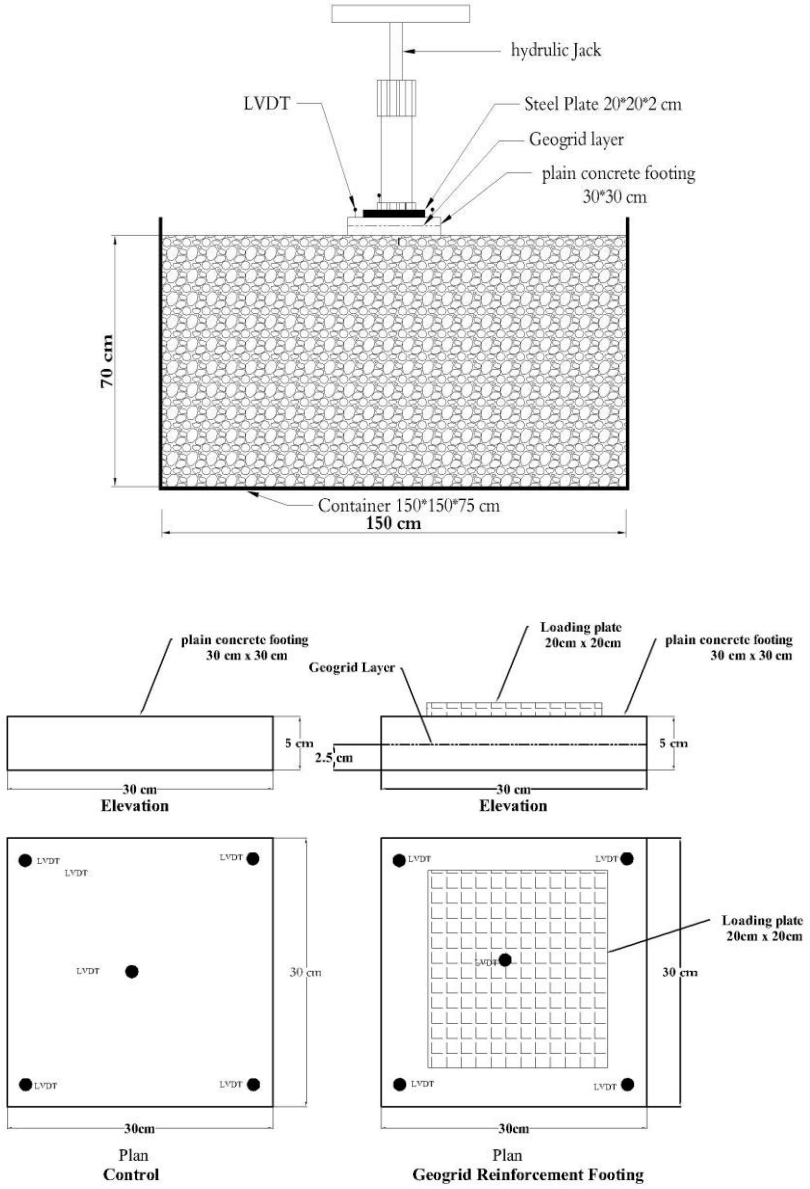

Fig.1: Illustration of Loading Position and Reinforcement Layout in a Typical Longitudinal Section.

2.1 Geogrid Properties

In this study, we analyzed the performance of various rigid geogrids, all of which were constructed from geosynthetic material but differed in terms of aperture

geometry and mechanical properties as reported by the manufacturer. Our findings are presented in Table 2. It is worth noting that the geogrids we used in our study were carefully selected based on their suitability for the intended application. Specifically, we examined both triaxial and biaxial geogrids, both of which were constructed from high-quality polypropylene.

Table 2. Product Specification of the geogrids used

Type	Structural integrity for Triaxial geogrid	Value
Tx 130	Junction Efficiency	93 %
	Aperture stability kg-cm/deg @ 5.0 kg-cm	3 kg-cm/deg
	Radial Stiffness at Low Strain @ 0.5% Strain	200 Kn/m
Tx 150	Junction Efficiency	93 %
	Overall Flexural Rigidity	750,000 mg.cm
	Radial Stiffness at Low Strain @ 0.5% Strain	300 Kn/m
Tx 160	Junction Efficiency	93 %
	Radial Stiffness at Low Strain @ 0.5% Strain	325 Kn/m

Component of Biaxial geogrid			
Mechanical properties	**Type of Geogrid**		**Unit**
	SS30	**SS40**	
Max tensile strength	30	40	Kn/m
Tensile Strength at 2% Strain	10.5	14	Kn/m
Tensile Strength at 5% Strain	21	28	Kn/m
Approx. strain at max tensile strength	11	11	%

2.2 Concrete mix proportions

The materials used in all the concrete mixes included CEM I Portland Cement 42.5 N, natural sand, and 12.5-5 mm gravel, with tap water used as the mixing medium. Two control mixes were used, labeled Control 1 and Control 2. Control 1 had a total water-cement ratio of 0.8 and consisted of 250 kg/m3 of Portland cement, 888.68 kg/m3 of sand, 954.75 kg/m3 of gravel, and 200 kg/m3 of water. Control 2 was made with Fiber glass reinforced concrete (FGRC) and had a ratio of 900 g/m3. The target 28 day mean compressive strength was 12 MPa, which is typical of mixes used for plain concrete footings in Egypt. A pan mixer of 0.1 m3 capacity was used to mix the materials, with the gravel placed first, followed by sand and cement. The dry mixing process lasted for one minute before adding water, and the mixing continued for an additional four minutes before the fibers were introduced.

2.3 Specimen Fabrication

The construction process for a plain concrete footing with a single layer of reinforcement is illustrated in Figure 2. Initially, a 2.5 cm layer of concrete was poured into the footing mold and thoroughly compacted. Subsequently, a geogrid layer was meticulously positioned, followed by another layer of concrete mixture. The consolidation process was meticulously carried out to ensure optimal

intermixing between the concrete layers above and below the geogrid. Upon demolding the specimens, no signs of surface cavities or separation were observed.

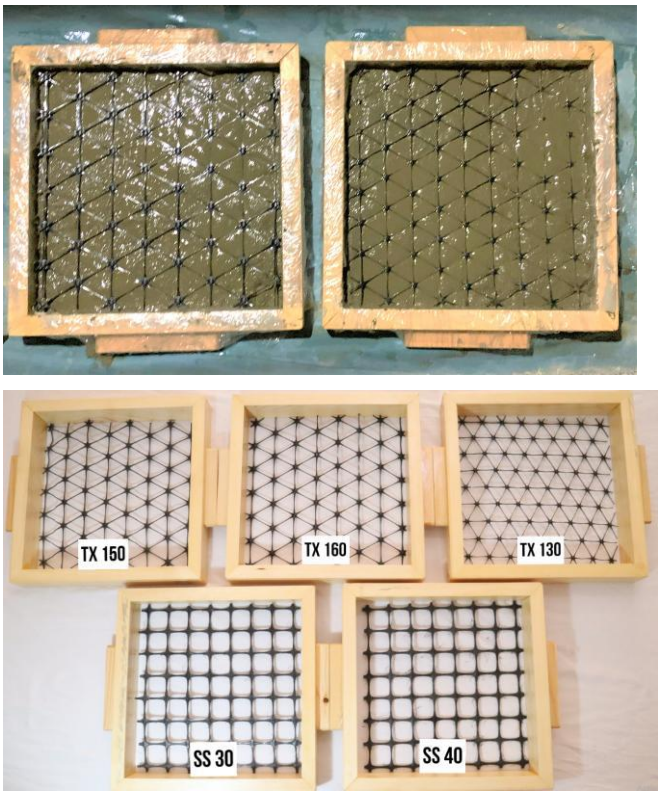

Fig.2. Placing of the geogrid layer after pouring and compacting of the 2.5 cm concrete layer,

2.4 Comprehensive Analysis of Soil Specifications

The composition of the foundation soil was a ratio of 2 parts gravel to 1 part sand. The soil utilized in this study conforms to the well-graded gravel with sand classification in accordance with the unified soil classification system. The uniformity coefficient and uniformity curvature, two critical indices to determine the soil grading, were determined as 22.50 and 1.98, respectively. The particle size distribution curve of the soil, as presented in Figure 3. Moreover, to evaluate the compaction characteristics of the soil, the standard proctor test was conducted, which is a standardized method in geotechnical engineering. The results indicate that the maximum dry density and the optimum moisture content were 2.078 t/m^3 and 6.88%, correspondingly. The corresponding dry density and moisture content curves of the proctor test are exhibited in Figure 4, which provide a graphical representation of the compaction characteristics of the soil. These thorough test results and analyses are critical in determining the soil's suitability for use under the footings.

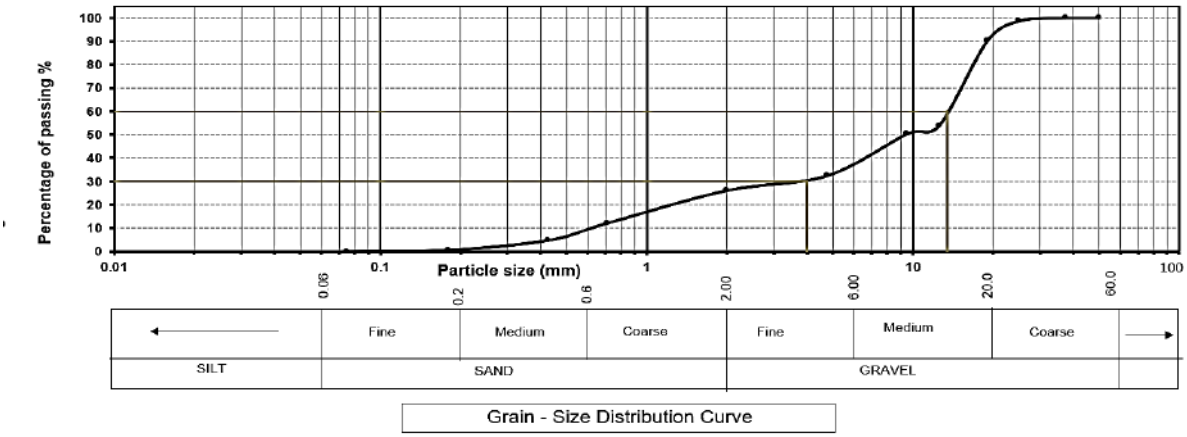

Fig.3: The particle size distribution curve for the soil used.

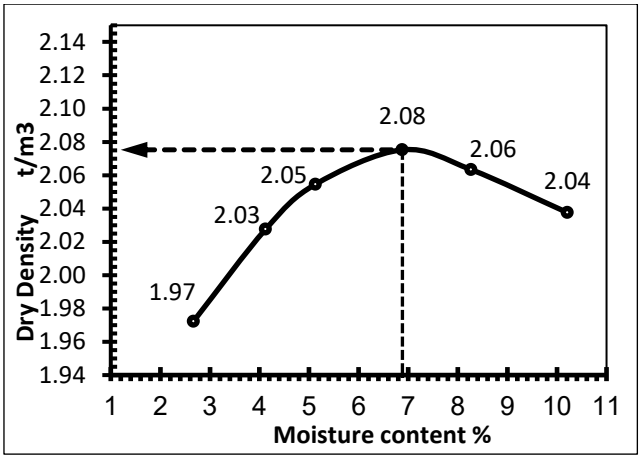

Fig.4: Relationship between dry density and moisture content for the soil used.

2.5 Experimental set-up and instrumentations

The study was conducted in a laboratory using a model setup consisting of a stiff test tank, a loading mechanism, a plate with sensors, and a system for collecting data. The test tank was designed to be large enough to fit the footing without the tank boundaries significantly affecting the soil stresses and strains. The tank was made of rigid steel with a length, width, and height of 1.50 m, 1.50 mm, and 0.70 m, respectively. A motorized 10-ton hydraulic jack applied a constant load to the footing, which was measured using a 1000 kN capacity load cell placed on top of the footing. To measure any vertical displacement, five LVDT transducers with a minimum resolution of 0.04 mm were placed at different locations on top of the footing. The output voltage of each electrical measuring circuit was automatically recorded at one-minute intervals using a data logging system. Figure 5 shows the principal dimensions and layout of the apparatus.

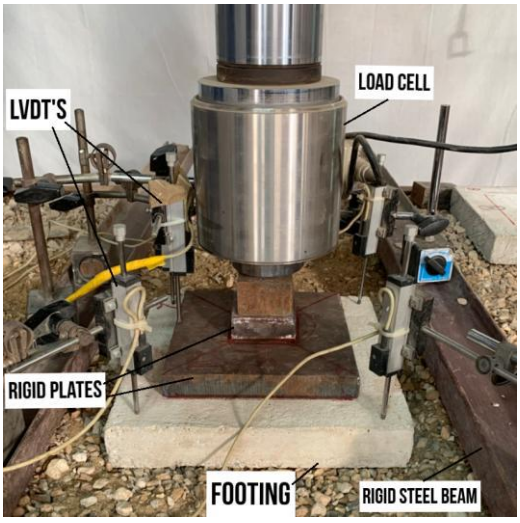

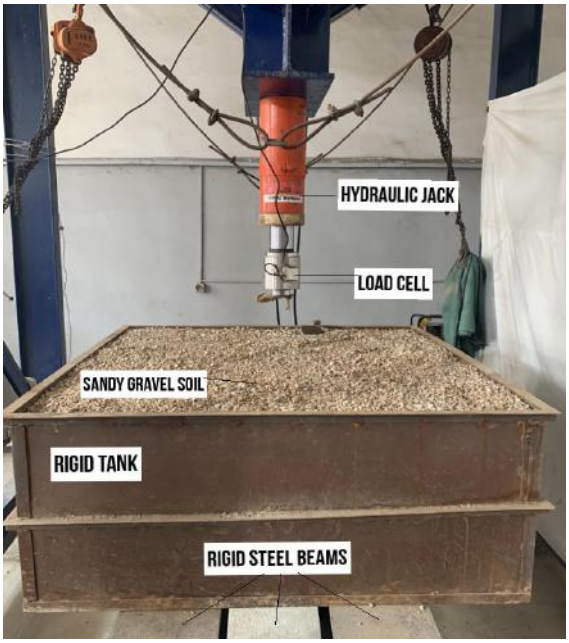

Fig 5: Model Setup and Apparatus Layout.

III. ANALYSIS OF EXPERIMENTAL PLAIN CONCRETE FOOTING RESULTS

3.1 General

An organizational chart has been included to streamline the presentation of the analysis of experimental plain concrete footing results. This chart serves as a visual guide, simplifying the structure of the analysis by breaking down its various components and findings, Fig. 6.

Load-deflection curves for plain concrete footings containing one layer of triaxial or biaxial geogrids are shown in Fig 7. Based on the obtained Figure, the load [P], vertical displacement [Δ] and Stiffness [K] were determined at first crack stage, yield stage and ultimate stage for all studied footings. Also, ductility [μ] and energy absorption [En] were obtained for each footing, Table 3.

We can see that using the geogrid on plain concrete footing affected the load-deflection behavior of the plain concrete footing significantly for the used geogrid types. It was observed that using biaxial geogrid has a good effect on the load-deflection behavior followed by triaxial geogrids. This could be because biaxial geogrids have higher tensile strength than triaxial geogrids.

The difference between biaxial and triaxial geogrids is the existence of a cord in the triaxial geogrid that divides the opening to two triangles and

causes the interlock cement matrix block volume to reduce.

3.2 Only Effect of Geogrid's on Footing Performance.

The load - deflection curves of reinforced and unreinforced concrete footings are presented in Fig. 7. Results show excellent repeatability of the tests, as well as the increase in peak load of reinforced concrete footings with geogrid compared to unreinforced concrete footing footings, Table 3. Results of unreinforced concrete footings show that specimens failed in a brittle mode immediately after peak, reaching peak loads of 56.66 and 59.924 kN at failure for P1 and P7.

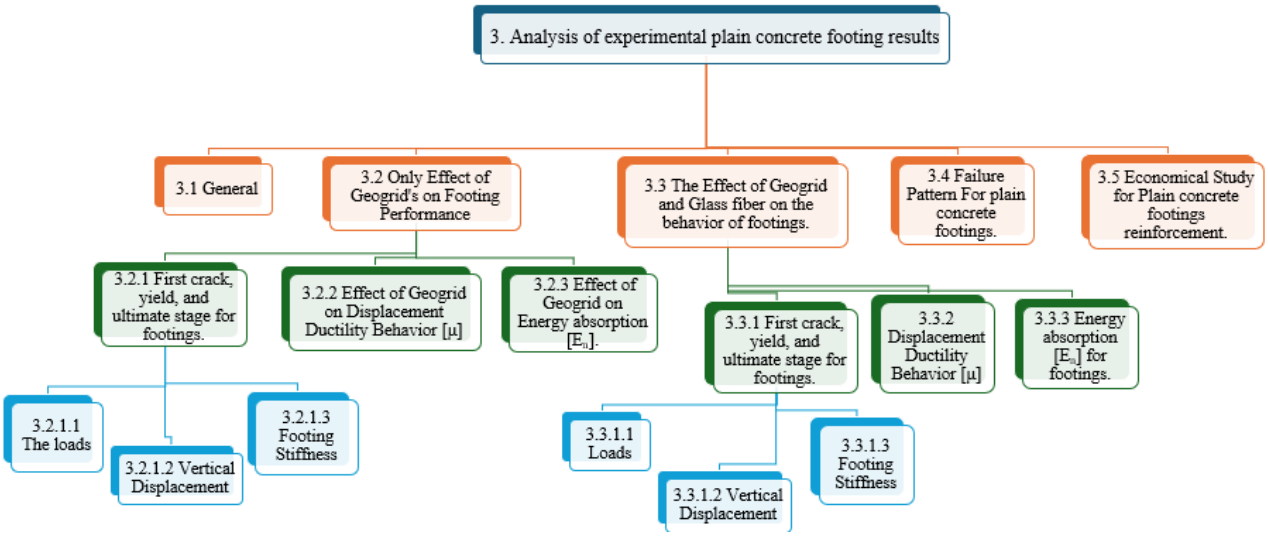

Fig. 6: Organizational Chart for Analysis of Experimental Plain Concrete Footing Results.

Table 3: Studied parameters for all footings

	First crack stage			Yield stage			Ultimate load stage			Ductility factor (μ)	Energy absorption (kN/mm)
	P_f (kN)	Δ_f (mm)	K_f (kN/mm)	P_y (kN)	Δ_y (mm)	K_y (kN/mm)	P_u (kN)	Δ_u (mm)	K_u (kN/mm)		
p1	45.000	8.890	5.062	51.562	11.470	4.495	56.659	15.902	3.563	1.386	640.953
p2	50.000	9.200	5.435	58.044	13.980	4.152	61.511	22.682	2.712	1.622	1064.712
p3	58.000	10.500	5.524	62.264	14.295	4.356	64.590	23.876	2.705	1.670	1155.020
p4	60.000	11.000	5.455	65.170	14.621	4.457	68.076	25.030	2.720	1.712	1335.254
p5	68.000	13.312	5.108	71.000	17.050	4.164	75.098	35.955	2.089	2.109	2272.243
p6	72.000	14.000	5.143	77.969	18.368	4.245	80.462	39.230	2.051	2.136	2524.678
p7	47.000	8.500	5.529	53.744	11.169	4.812	59.924	17.930	3.342	1.605	783.326
p8	53.000	9.013	5.880	59.000	12.631	4.671	65.489	23.353	2.804	1.849	1180.890
p9	60.000	9.800	6.122	64.510	13.633	4.732	66.460	25.222	2.635	1.850	1285.978
p10	61.000	10.000	6.100	67.335	14.103	4.775	70.849	27.060	2.618	1.919	1548.118
p11	70.000	11.200	6.250	72.707	15.641	4.648	78.656	36.489	2.156	2.333	2398.492
p12	74.000	12.693	5.830	79.121	16.813	4.706	82.638	41.391	1.997	2.462	2907.221

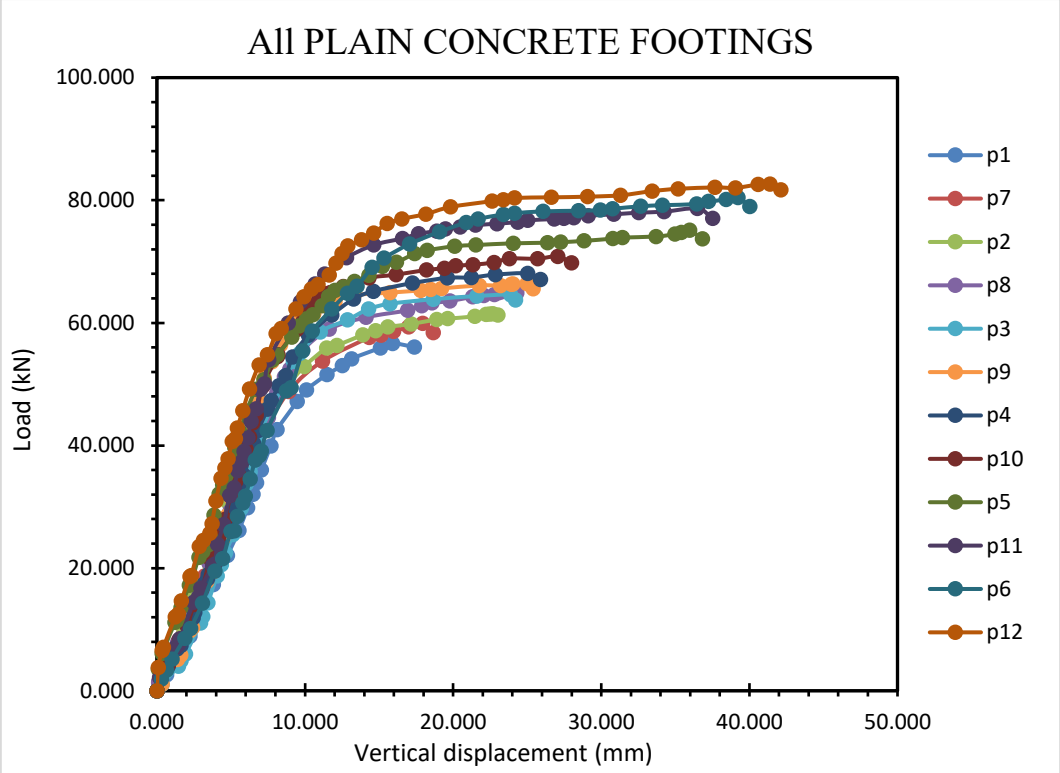

Fig. 7: Load-deflection curves for all plain concrete footings.

On the other hand, the load-deformation curves of reinforced-concrete specimens exhibited delayed failure and extra peak load in all cases. After load drop, reinforced geogrid footings gained post cracking ductility until cracks reached top surface footings, where failure was completed, Fig. 8. Similar behavior was evidenced in the research of Meski et al. (2013) [81] using Biaxial and Triaxial geogrids, and in the research of Meng et al. (2019) [95], although this last used Biaxial geogrids in pervious concrete beams.

At this point, each specimen was compared to its control in order to extract the influence of the geogrid's presence within the footings independently. The following variables have been investigated:

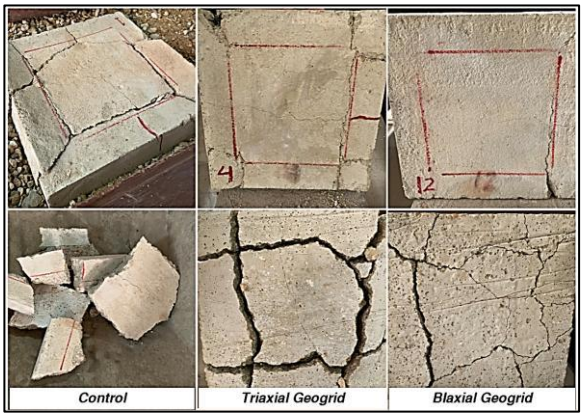

Fig. 8: Failure and cracking mode for control, triaxial and biaxial geogrid footings.

3.2.1 Effect of Geogrid on First crack, yield, and ultimate stage for footings.

For all footing, linear load–deflection curves were found even after the initial cracks appeared at the bottom along the sides of the footing. As the cracks developed upward to the top surface, the curves showed a non-linear behavior. It was found that the reinforcement would delay the onset of initial cracks, but the post-crack behavior of the

reinforcement footings demonstrated higher load-carrying capacities than the plain concrete footing.

3.2.1.1 The loads

As compared to a plain concrete foundation, triaxial and biaxial reinforcing often results in gradual increases in the values of the cracking load (P_{fc}), yield load (P_y), and ultimate load (P_{ult}) as follows:

- P_{fc}, P_y and P_{ult} values at footings reinforced by triaxial geogrid Tx-130 increase by about average 11.93%,11.175% and 8.92% respectively than that for relative plain concrete footing.
- P_{fc}, P_y and P_{ult} values at footings reinforced by triaxial geogrid Tx-150 increase by about average 28.27%,20.39% and 12.45% respectively than that for relative plain concrete footing.
- P_{fc}, P_y and P_{ult} values at footings reinforced by triaxial geogrid Tx-160 increase by about average 31.56%,25.84% and 19.19% respectively than that for relative plain concrete footing.
- P_{fc}, P_y and P_{ult} values at footings reinforced by Biaxial geogrid SS30 increase by about average 50.02%,36.49% and 31.90% respectively than that for relative plain concrete footing.
- P_{fc}, P_y and P_{ult} values at footings reinforced by Biaxial geogrid SS40 increase by about average 58.44%,49.21% and 39.95% respectively than that for relative plain concrete footing.

Geogrid reinforcement effect: Cracking load (P_{fc}), yield load (P_y), and ultimate load (P_{ult}) increase with triaxial reinforcement by average percentages of 23.92%, 19.13%, and 13.52%, respectively. Similar improvements are observed with biaxial reinforcement, with average percentages of 54.23%, 42.85%, and 35.92% for cracking load, yield load, and ultimate load, respectively.

3.2.1.2 Vertical Displacement

Based on the obtained results, it can be inferred that.

- Δ_{fc}, Δ_y and Δ_{ult} values at footings reinforced by triaxial geogrid Tx-130 increase by about average 4.76%,17.48% and 36.44% respectively than that for relative plain concrete footing.
- Δ_{fc}, Δ_y and Δ_{ult} values at footings reinforced by triaxial geogrid Tx-150 increase by about average 16.70%,23.34% and 45.41% respectively than that for relative plain concrete footing.
- Δ_{fc}, Δ_y and Δ_{ult} values at footings reinforced by triaxial geogrid Tx-160 increase by about average 20.69%,26.87% and 54.16% respectively than that for relative plain concrete footing.
- Δ_{fc}, Δ_y and Δ_{ult} values at footings reinforced by Biaxial geogrid SS30 increase by about average 40.75%,44.34% and 114.81% respectively than that for relative plain concrete footing.
- Δ_{fc}, Δ_y and Δ_{ult} values at footings reinforced by Biaxial geogrid SS40 increase by about average 53.40%,55.33% and 138.78% respectively than that for relative plain concrete footing.

As compared to a plain concrete footing, triaxial and biaxial reinforcing often results in gradual increases in the values of vertical displacement at cracking stage ($\boldsymbol{\Delta}_{fc}$), yield stage ($\boldsymbol{\Delta}_y$), and ultimate stage ($\boldsymbol{\Delta}_{ult}$).

3.2.1.3 Footing Stiffness

As compared to a plain concrete foundation, triaxial and biaxial reinforcing often results in gradual increases in the value of the stiffness at cracking stage (K_{fc}) and decrease in the value of stiffness at yield stage (K_y), and ultimate stage (K_{ult}) as follows:

- K_{fc} values at footings reinforced by triaxial geogrid Tx-130 increase by about average 6.85% than that for relative plain concrete footing. While K_y and K_{ult} decrease by about 5.28% and 19.99% respectively than that for relative plain concrete footing.
- K_{fc} values at footings reinforced by triaxial geogrid Tx-150 increase by about average 9.92% than that for relative plain concrete footing. While K_y and K_{ult} decrease by about 2.38% and 22.61% respectively than that for relative plain concrete footing.

- K_{fc} values at footings reinforced by triaxial geogrid Tx-160 increase by about average 9.038% than that for relative plain concrete footing. While K_y and K_{ult} decrease by about 0.8% and 22.70% respectively than that for relative plain concrete footing.
- K_{fc} values at footings reinforced by Biaxial geogrid SS30 increase by about average 6.97% than that for relative plain concrete footing. While K_y and K_{ult} decrease by about 5.38% and 38.44% respectively than that for relative plain concrete footing.
- K_{fc} values at footings reinforced by Biaxial geogrid SS40 increase by about average 3.5% than that for relative plain concrete footing. While K_y and K_{ult} decrease by about 3.88% and 41.35% respectively than that for relative plain concrete footing.

Triaxial geogrid reinforcement induces changes in stiffness: k_{fc} increases by average 8.6%, while k_y and k_{ult} decrease by average 2.82% and 21.76%. Similarly, biaxial geogrid reinforcement: k_{fc} increases by average 5.23%, while k_y and k_{ult} decrease by average 4.63% and 39.89%.

The experimental results reveal that during the First crack stage, an increase in load causes a corresponding increase in displacement, albeit not in a proportional manner, and an increase in stiffness, although not to the same extent as load and displacement. During the yield stage, an increase in load leads to an increase in displacement that is equal to, and in some instances greater than, the increase in load, while the stiffness experiences a decrease, albeit with minimal magnitudes. At the ultimate stage, an increase in load results in a relatively low increase, whereas the displacement undergoes a more significant increase than the load, and the stiffness experiences a substantial decrease. These findings are also supported by Fig. 9 which describe the increases and decreases ratio for the studied parameters.

3.2.2 Effect of Geogrid on Displacement Ductility Behavior [μ]

In this study, we evaluated the effect of geogrid reinforcement on the displacement ductility behavior of concrete footings. The displacement ductility index, which represents the ability of the structural element to undergo large deflections without significant strength reduction before failure, was used to assess the performance of the concrete footings. To ensure concrete structures can withstand seismic events, they must maintain their strength above the yield strength up to the allowable plastic deformation adopted in the design [96].

Our findings show that the use of geogrid reinforcement can significantly improve the displacement ductility behavior of concrete footings, particularly for biaxial geogrids. The displacement ductility indexes were increased by 15.25% to 23.48% for the group of "tri-axial geogrid reinforcement," and by 45.33% and 54.06% for the group of "biaxial geogrid reinforcement" compared to the concrete control footings. Our study found a positive correlation between the increase in displacement ductility and the stiffness of triaxial geogrids for the "tri-axial geogrid reinforcement" group, and a strong positive correlation with the tensile strength of biaxial geogrids for the "biaxial geogrid reinforcement" group. These findings have important implications for the design of reinforced concrete structures in earthquake-prone regions, Fig. 10.

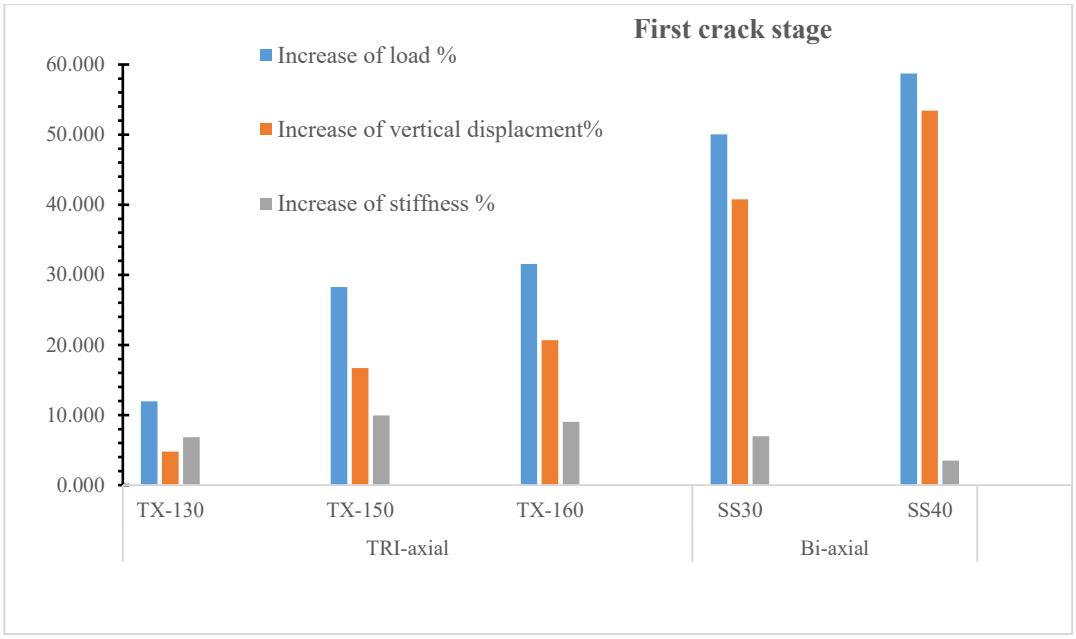

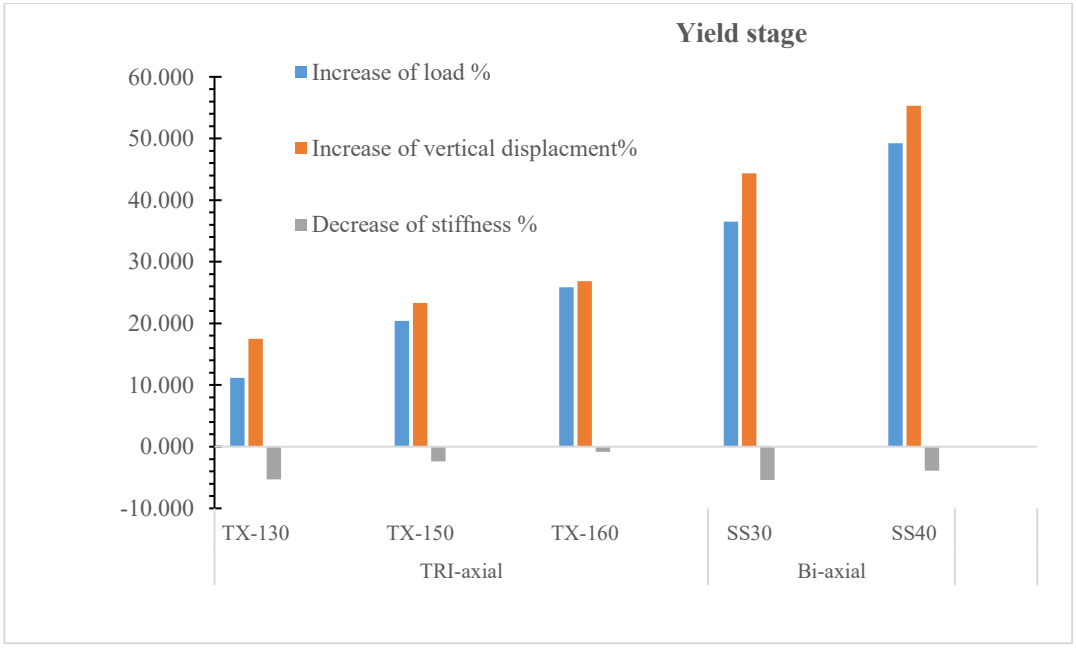

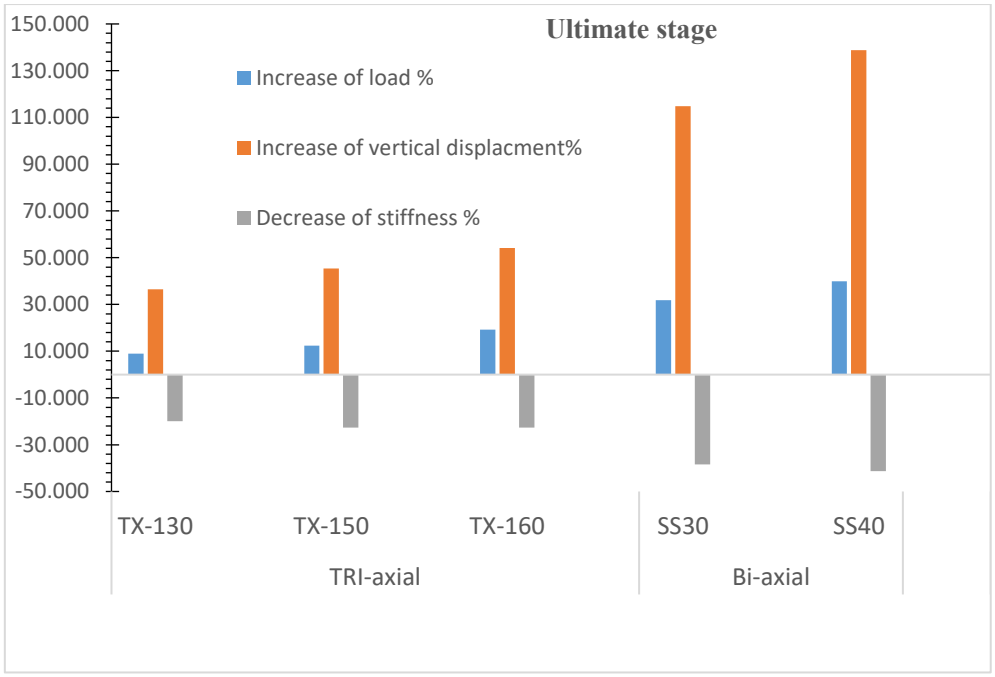

Fig.9: Effect of geogrid on First crack, yield, and ultimate stage for footings.

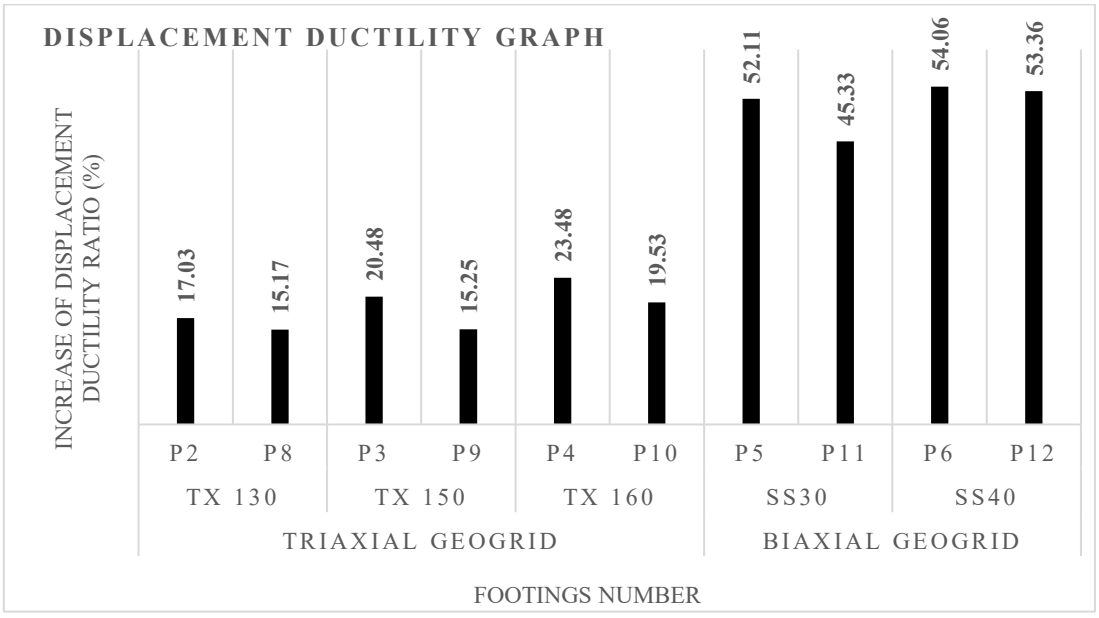

Fig. 10: Ratio of Increase in Displacement Ductility for Concrete Footings with Geogrid Reinforcement Compared to Control Footings.

Geogrid reinforcement substantially enhances concrete footing displacement ductility. On average, triaxial geogrids demonstrate a 19.37% increase, while biaxial geogrids exhibit a remarkable average improvement of 49.695% compared to control footings.

3.2.3 Effect of Geogrid on Energy absorption [E_n].

Considerable energy absorption ability is favorable in the case of large earthquakes under which significant energy absorption is required because a smaller energy dissipation results in a significant dynamic response and hysteretic damping of concrete structures during earthquakes. Energy absorption was calculated based on the area enclosed by the load-deflection curve. The behavior of the tested footings has also been compared in the

form of energy absorption capacity, which was calculated as the area under its load-deflection curves in Fig. 7.

The energy dissipation capacities were increased by a percent varying from 58.43% to 102.97% for group of triaxial geogrid reinforcement compared to the concrete control footing "P1 and P7" with a positive correlation to the stiffness of Triaxial geogrid, while it was increased by a percent equal to 230.35, and 282.516% for group of "Biaxial geogrid reinforcement", compared to the concrete control footings with a strong positive correlation to the tensile strength of biaxial geogrids. The biaxial geogrids with the ultimate tensile strength of 21 kN/m and 28 kN/m provide more efficient utilization as they had higher energy dissipation values when compared to the other geogrids' cases, Fig. 11.

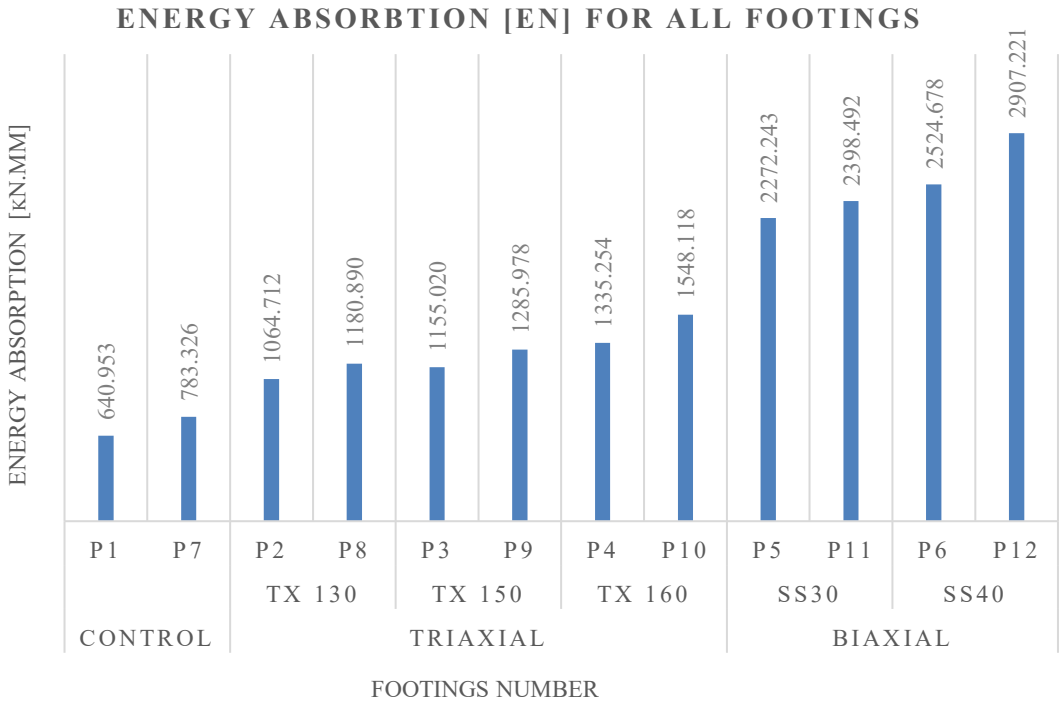

Fig.11: Absorption of Impact Energy across All Footings

Geogrid reinforcement substantially enhances energy absorption capacities. On average, triaxial geogrids experience a 77.8% increase, with positive stiffness correlation. Biaxial geogrids show an impressive average increase of 256.43%, strongly correlating with tensile strength.

3.3 The Effect of Geogrid and Glass fiber on the behavior of footings.

3.3.1 First crack, yield, and ultimate stage for footings.

It was found that the reinforcement footings by glass fiber and geogrid would delay the onset of initial cracks and the post-crack behavior of the reinforcement footings demonstrated higher load-carrying capacities than the plain concrete footing (P1).

3.3.1.1 Loads

As compared to a plain concrete foundation, triaxial and biaxial reinforcing with (GFRC) often results in gradual increases in the values of the cracking load (P_{fc}), yield load (P_y), and ultimate load (P_{ult}) as follows:

- P_{fc}, P_y and P_{ult} values at footings reinforced by triaxial geogrid Tx-130 increase by about average 17.77%,14.425% and 15.58% respectively than that for the concrete control footing (P1).
- P_{fc}, P_y and P_{ult} values at footings reinforced by triaxial geogrid Tx-150 increase by about average 33.33%,25.112% and 17.29% respectively than for the concrete control footing (P1).

- P_{fc}, P_y and P_{ult} values at footings reinforced by triaxial geogrid Tx-160 increase by about average 35.55%,30.59% and 25.04% respectively than that for the concrete control footing (P1).
- P_{fc}, P_y and P_{ult} values at footings reinforced by Biaxial geogrid SS30 increase by about average 55.55%,41.00% and 38.82% respectively than that for the concrete control footing (P1).
- P_{fc}, P_y and P_{ult} values at footings reinforced by Biaxial geogrid SS40 increase by about average 64.44%,53.44% and 45.85% respectively than that for the concrete control footing (P1).

The results indicate that the addition of glass fiber into the concrete mixture with geogrid reinforcement increase the load capacity at various stages, including the first crack, yield, and ultimate stages, when compared to the load capacity of geogrid reinforcement alone. This suggests that the composite material system exhibits superior performance compared to the geogrid reinforcement in isolation. Therefore, the utilization of glass fiber in concrete mixture along with geogrid reinforcement can effectively enhance the structural capacity of the composite material system.

3.3.1.2 Vertical Displacement

As compared to a plain concrete footing (P1), triaxial and biaxial reinforcing often results in gradual increases in the values of vertical displacement at cracking stage (Δ_{fc}), yield stage (Δ_y), and ultimate stage (Δ_{ult}) as follows:

- Δ_{fc}, Δ_y and Δ_{ult} values at footings reinforced by triaxial geogrid Tx-130 increase by about average 1.38%,10.12% and 46.86% respectively than that for the concrete control footing (P1).
- Δ_{fc}, Δ_y and Δ_{ult} values at footings reinforced by triaxial geogrid Tx-150 increase by about average 10.23%,18.85% and 58.61% respectively than that for the concrete control footing (P1).
- Δ_{fc}, Δ_y and Δ_{ult} values at footings reinforced by triaxial geogrid Tx-160 increase by about average 12.4%,22.95% and 70.17% respectively than that for the concrete control footing (P1).
- Δ_{fc}, Δ_y and Δ_{ult} values at footings reinforced by Biaxial geogrid SS30 increase by about average 25.98%,36.36% and 129.46% respectively than that for the concrete control footing (P1).
- Δ_{fc}, Δ_y and Δ_{ult} values at footings reinforced by Biaxial geogrid SS40 increase by about average 42.7%,46.58% and 160.29% respectively than that for the concrete control footing (P1).

The study found that incorporating glass fibers into the concrete mixture in the presence of geogrid was effective in reducing vertical displacement during the initial cracking and yield stages. However, once the geogrid began to elongate, a significant increase in vertical displacement values was observed. This behavior can be attributed to the reduced effectiveness of the glass fibers in resisting crack formation under high stress conditions.

3.3.1.3 Footing Stiffness

In comparison to plain concrete footing, the incorporation of triaxial and biaxial reinforcement frequently leads to a gradual augmentation in the stiffness parameters at both cracking stage (k_{fc}) and yield stage (k_y), while the stiffness value at ultimate stage (K_{ult}) is decreased as follows.

- k_{fc} and k_y values at footings reinforced by triaxial geogrid Tx-130 increase by an average of 16.17% and 3.90% respectively, then that for the concrete control footing (P1). k_{ult} decreases by about 21.29% less than that for the concrete control footing (P1).
- k_{fc} and k_y values at footings reinforced by triaxial geogrid Tx-150 increase by an average of 20.5% and 5.26% respectively, then that for the concrete control footing (P1). k_{ult} decreases by about 26% less than that for the concrete control footing (P1).
- k_{fc} and k_y values at footings reinforced by triaxial geogrid Tx-160 increase by an average of 20.9% and 6.20% respectively, then that for the concrete control footing (P1). k_{ult} decreases by about 26.52% less than that for the concrete control footing (P1).

- k_{fc} and k_y values at footings reinforced by biaxial geogrid SS30 increase by an average of 23.47% and 3.40% respectively, then that for the concrete control footing (P1). k_{ult} decreases by about 39.50% less than that for the concrete control footing (P1).
- k_{fc} and k_y values at footings reinforced by biaxial geogrid SS40 increase by an average of 15.17% and 4.68% respectively, then that for the concrete control footing (P1). k_{ult} decreases by about 43.96% less than that for the concrete control footing (P1).

The results indicate that the addition of glass fibers significantly improves the stiffness of the concrete mixture during the yield stages when compared to geogrids alone. This implies that the inclusion of fibers, in conjunction with geogrids, plays a crucial role in improving the behavior of plain concrete footing bases, Fig. 12.

These findings are significant for the civil engineering industry as they offer valuable insights into the use of glass fibers as a reinforcing material in the construction of structures that require enhanced load-bearing capacities. Further research could explore the effects of varying fiber concentrations and mix proportions on the stiffness properties of concrete mixtures to optimize the benefits of this approach.

3.3.2 Effect of Geogrid and Glass fibers on Displacement Ductility Behavior [μ]

The displacement ductility indexes were increased by a percent varying from 33.36% to 38.40% for group of "tri-axial geogrid reinforcement" compared to the concrete control footing "P1" with a positive correlation to the stiffness of Triaxial geogrid, while it was increased by a percent equal to 68.27%, and 77.57% for group of "Biaxial geogrid reinforcement", compared to the concrete control footing "P1" with a strong positive correlation to the tensile strength of biaxial geogrids, Fig. 13.

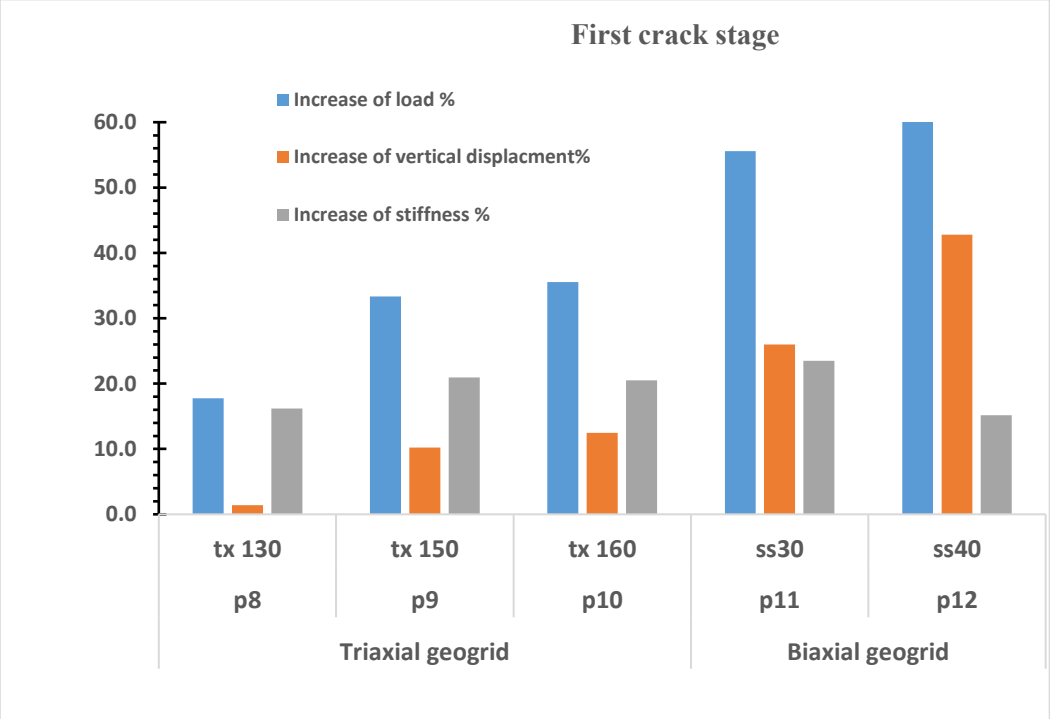

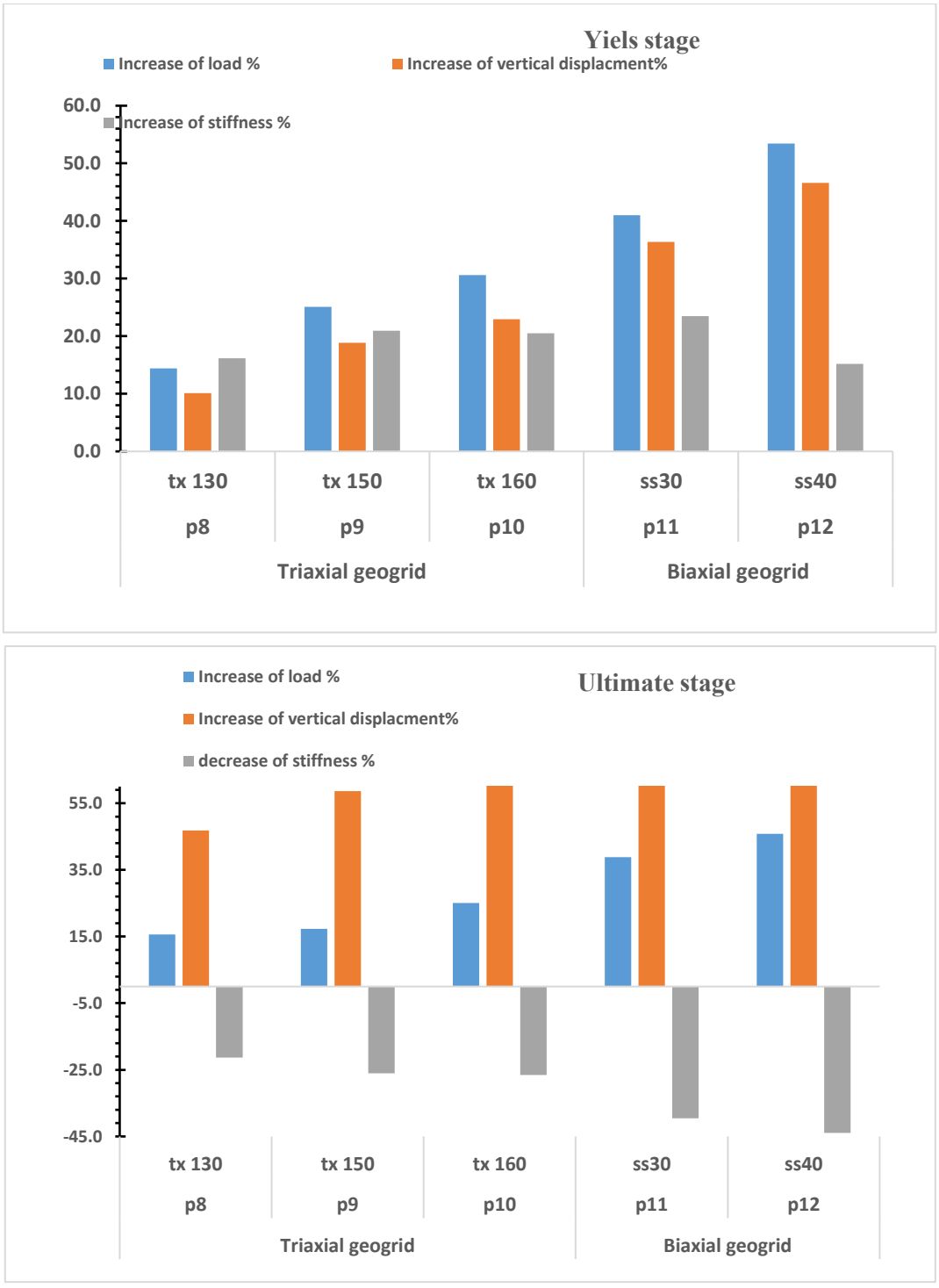

Fig. 12: Effect of geogrid and glass fiber on First crack, yield, and ultimate stage for footings

3.3.3 Effect of Geogrid and Glass fibers on Energy absorption [E_n] for footings.

The energy dissipation capacities were increased by a percent varying from 84.24% to 141.53% for group of "tri-axial geogrid reinforcement" compared to the concrete control footing "P1" with a positive correlation to the stiffness of Triaxial geogrid, while it was increased by a percent equal to 274.20%, and 353.57% for group of "Biaxial geogrid reinforcement", compared to the concrete control footing with a strong positive correlation to the tensile strength of biaxial geogrids, Fig. 14.

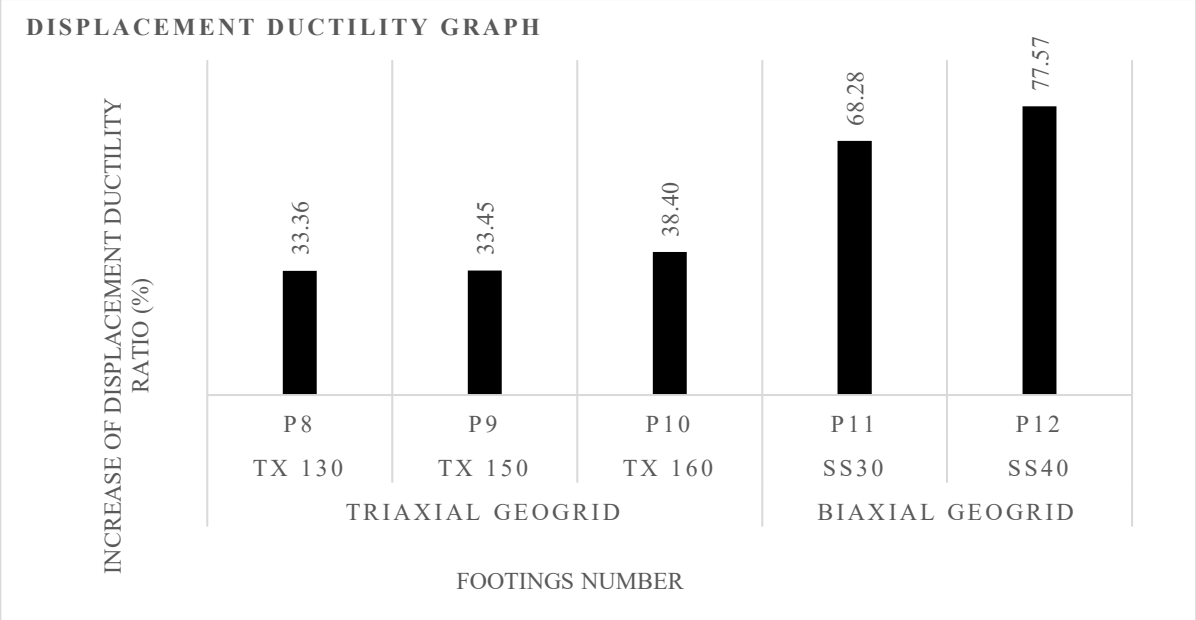

Fig. 13: Ratio of Increase in Displacement Ductility for Concrete Footings with Geogrid and glass fiber Reinforcement Compared to Control Footing (P1).

Geogrid reinforcement with (GFRC) substantially enhances concrete footing displacement ductility. On average, triaxial geogrids demonstrate a 35.07% increase, while biaxial geogrids exhibit a remarkable average improvement of 72.9% compared to control footings.

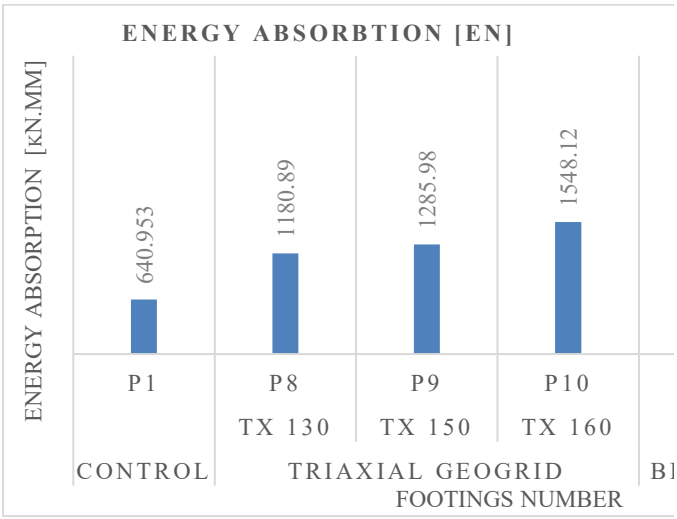

Fig. 14: Comparison of Impact Energy Absorption of Footings Reinforced with Geogrid and Glass Fiber versus Control Footing (P1).

Geogrid reinforcement with (GFRC) substantially enhances energy absorption capacities. On average, triaxial geogrids experience a 108.8% increase, with positive stiffness correlation. Biaxial geogrids show an impressive average increase of 313.88%, strongly correlating with tensile strength.

3.4 Failure Pattern For plain concrete footings.

From the experimental observation, there are two types of failure mode. For specimens without geogrid reinforcement "control specimens", the specimens broke into many pieces at failure. During the initial loading, the crack developed along the middle of the specimens' bottom surface area. For the specimens without reinforcement, the specimens will crack first then break into many pieces at ultimate failure.

Fig. 15 shows the failure mode of the control specimen where it was separated into many pieces. During the experimental process, after the first crack developed the specimen started to deflect when under loading. More cracks developed perpendicular to the failure crack after the first crack developed. The concrete was no longer able to resist more loading as there is no bonding at the crack area. After increasing the load, the specimen fails ultimately without reinforcement. The control specimen is unable to sustain more loading and hence fails in a short period.

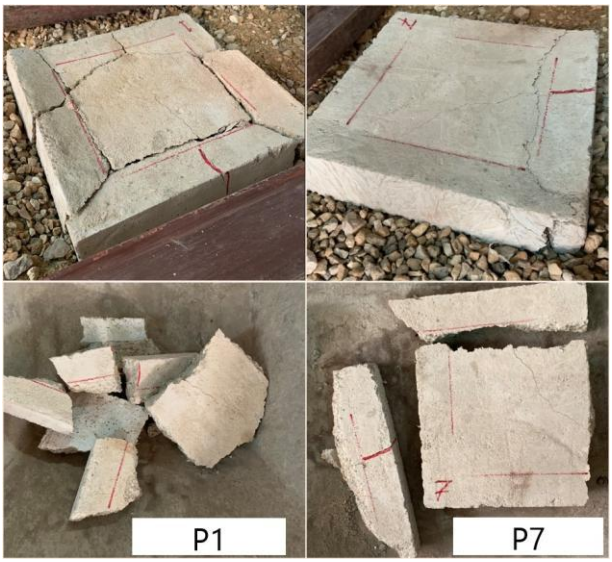

Fig. 15: Failure Pattern for control footings P1 and P7

Furthermore, the specimens were reinforced with a geogrid; the failure mode was totally different from the first failure mode as mentioned previously. For geogrid reinforced specimens, the specimens did not break into pieces at ultimate failure. From the experimental observation, the specimens reinforced with a geogrid were able to sustain slightly more loading before the first crack developed. The geogrid addition was a greater feature in concrete to resist loading.

Fig. 4.16 and 4.17 shows the cracks development on specimen reinforced with geogrid. The crack development was seen in an all-directional pattern. This means that the geo grid affected the contribution in the distribution of the impact energy throughout the concrete surface instead of only one direction. Where the impact energy was divided into lesser magnitude for both directions.

Additionally, geogrid contributed to crack development control, where the impact energy tends to travel through it instead of a random direction, causing development of the crack along the direction of reinforcement. A triaxial geogrid in comparison to biaxial geogrids, may reveal greater cracks, according to our study.

The experiments have shown that the addition of glass fiber to concrete has a significant impact on the crack pattern of concrete specimens. The research found that when added in the correct proportion, glass fibers can increase the tensile strength of the concrete, which results in reduced cracking. The study also found that the fibers act as a reinforcement that prevents the propagation of cracks and improves the durability of the concrete. Additionally, the research showed that the use of glass fibers promotes a more uniform distribution of cracks in the concrete, resulting in an improved aesthetic appearance. Overall, the results of this research study suggest that incorporating glass fibers into concrete can result in a stronger, more durable material with a more desirable crack pattern.

4.5 Economical Study for Plain concrete footings reinforcement.

A comprehensive analysis of reinforcement costs is outlined in Table 4. The percentage shift in Reinforcement prices, relative to p1, has been meticulously computed and tabulated in Table 4. Furthermore, the correlation between the escalation in the price ratio attributed to reinforcement and the corresponding increments in load ratios at each stage is visually represented in Fig. 18.

Incorporating glass fiber bristles and geogrid into plain concrete yields notable enhancements, as evidenced by the following outcomes: The results demonstrate a potential escalation in the load at first crack, ranging from 17.78% to 64.44% compared to the load observed in footing (P1). Similarly, the yield load exhibits an increase within the range of 14.43% to 53.45% relative to the yield in footing (p1).

Moreover, the ultimate load showcases an augmentation ranging from 15.58% to 45.58% in comparison to the ultimate load in control footing (P1). It's worth noting that these substantial advancements come at the expense of an elevated cost, varying from 119.25% to 153% when compared to the price of a control plain concrete footing.

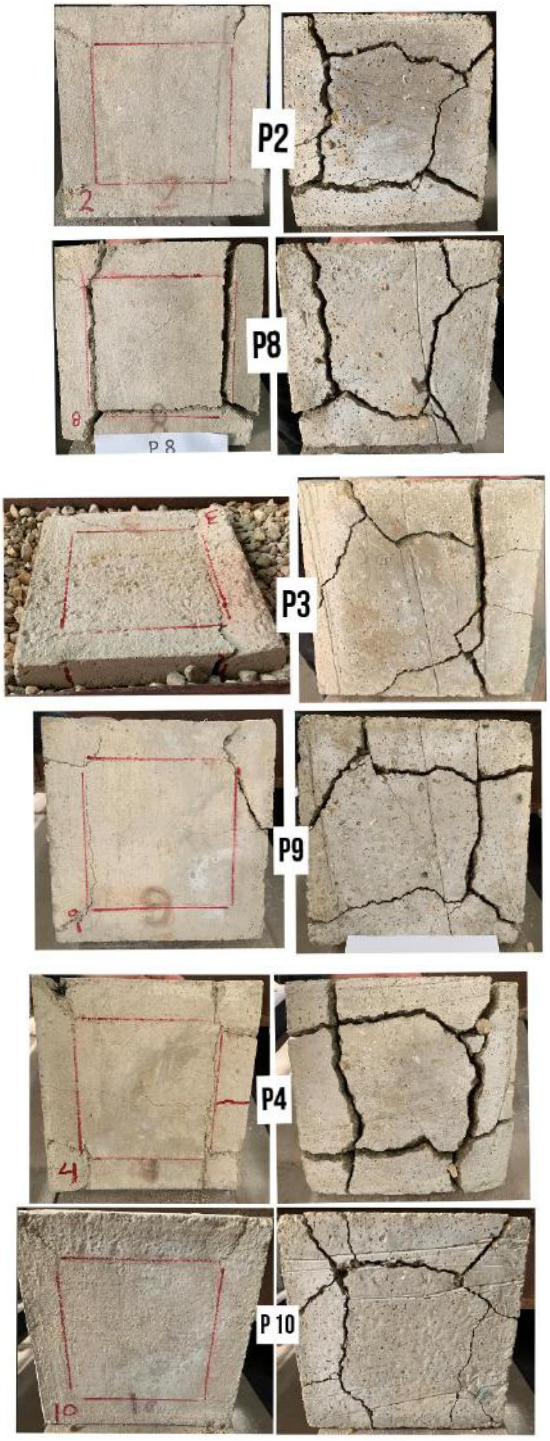

Fig. 4.16: Failure Pattern for Triaxial geogrid reinforcement footings.

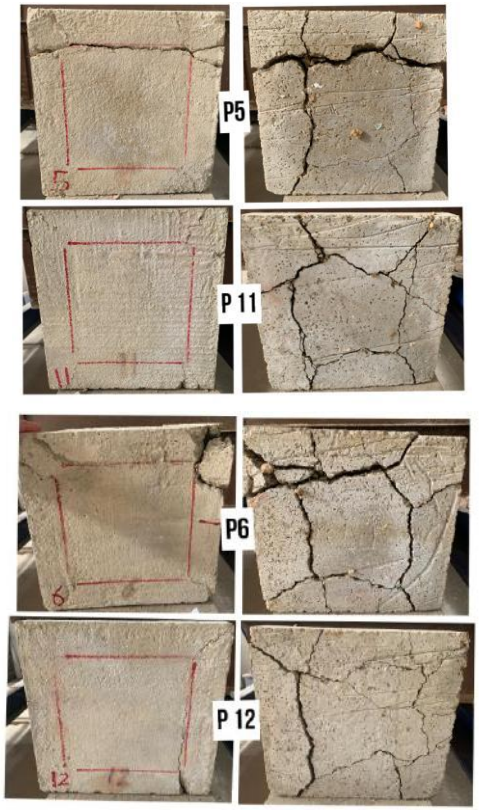

Fig. 4.17: Failure Pattern for Biaxial geogrid reinforcement footings.

Table 4: Percentage Change in Reinforcement Prices Compared to p1.

Geogrid type	Footing Number	Ratio increases on $P_{f.c}$	Ratio increases on P_y	Ratio increases on P_u	Total Price of specimen (E.G.P)	Ratio increases on price (E.G.P)
-	P1	-	-	-	4	-
All footings compared to control footing (P1)						
TX130	P8	17.78%	14.43%	15.58%	8.77	119.25%

Tx150	P9	33.33%	25.11%	17.30%	9.67	141.75%
Tx160	P10	35.56%	30.59%	25.04%	10.57	164.25%
SS30	P11	55.56%	41.01%	38.82%	9.22	130.50%
SS40	P12	64.44%	53.45%	45.85%	10.12	153.00%

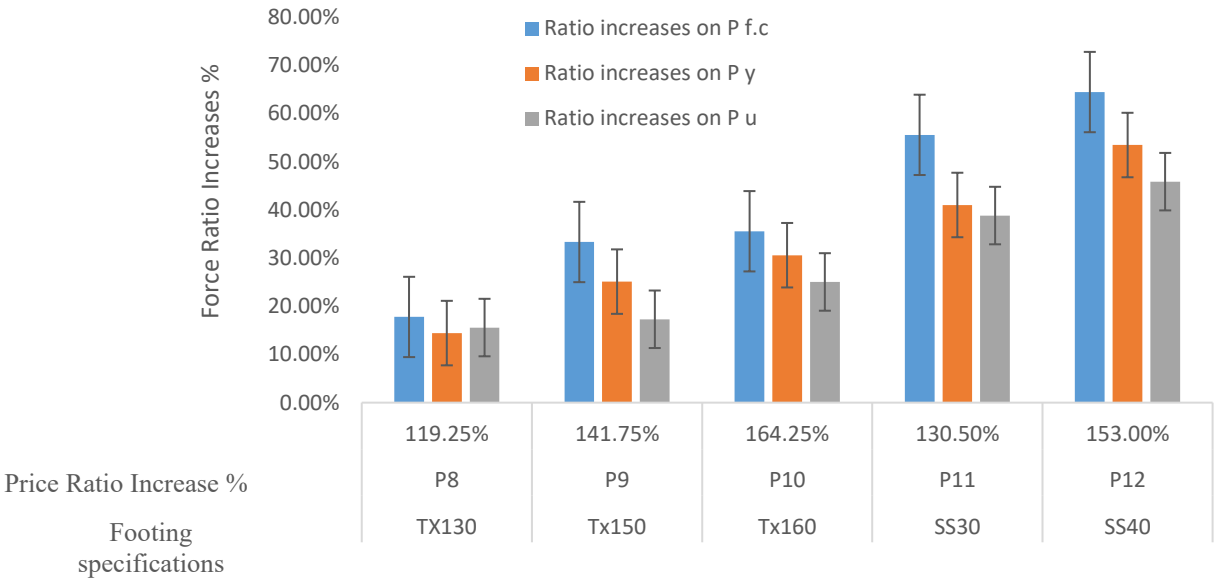

Fig.18: Relationship Between Price Ratio Escalation due to Reinforcement and specimen Number for Tested footing specimens.

IV. CONCLUSION

Based on the research work, the following conclusions can be summarized:

1- Both triaxial and biaxial geogrid reinforcement significantly enhances structural performance, increasing cracking load (P_{fc}), yield load (P_y), and ultimate load (P_{ult}) for plain concrete footings.
2- Geogrid reinforcement, whether in the form of biaxial or triaxial reinforcement, influences stiffness by increasing k_{fc} and decreasing k_y and k_{ult}.
3- Geogrid reinforcement significantly improves energy absorption capacity and displacement ductility behavior for plain concrete footings. Triaxial geogrids exhibit positive stiffness correlation, while biaxial geogrids demonstrate a strong correlation with tensile strength, resulting in substantial increases.
4- Geogrid reinforcement with (GFRC) consistently enhances load capacities in plain concrete footings. Triaxial geogrids yield increases for P_{fc}, P_y, and P_{ult}, while biaxial geogrids exhibit substantial improvements in these load capacities.
5- Geogrid reinforcement with (GFRC) consistently influences stiffness in concrete footings. geogrid reinforcement leads to increases in k_{fc} and k_y, but a decrease in k_{ult}. The specific values for these changes vary between biaxial and triaxial geogrids, with both showing improvements in stiffness.
6- Geogrid reinforcement with (GFRC) significantly improves concrete plain concrete footing performance. Triaxial and biaxial geogrids both show substantial enhancements in displacement ductility and energy absorption compared to control footings. Adding glass fiber bristles played a role in enhancing these values.
7- Geogrid reinforcement for plain concrete footings reduces concrete failure, averting fragmentation. Enhanced impact resistance and controlled cracks were seen. Triaxial geogrids may yield more cracks than biaxial, yet both enhance controlled crack growth, boosting stability.

8- Biaxial geogrids outperform triaxial ones in strengthening plain concrete footings. Furthermore, their cost effectiveness enhances this advantage.

REFERENCES

[1] Tang X, Chehab GR, Kim S. Laboratory study of geogrid reinforcement in Portland cement concrete. RILEM Int Conf Cracking Pavements 2008;2008:769–78.

[2] Meski F, Chehab G. Flexural behavior of concrete beams reinforced with different types of geogrids. J Mater Civil Eng 2013;26(8):04014038.

[3] Sivakamasundari S, Daniel AJ, Kumar A. Study on flexural behavior of steel fiber RC beams confined with biaxial Geo-Grid. Procedia Eng 2017;173:1431–8.

[4] Mittal RK, Gill G. Sustainable application of waste tire chips and geogrid for improving load carrying capacity of granular soils. J Cleaner Prod 2018;200: 542–51.

[5] Itani H, Saad G, Chehab G. The use of geogrid reinforcement for enhancing the performance of concrete overlays: An experimental and numerical assessment. Constr Build Mater 2016;124:826–37.

[6] El-Kasaby, E. S. A., Roshdy, M., Awwad, M., & Abo-Shark, A. A. (2023). Enhancing Flexural Performance of GFRC Square Foundation Footings through Uniaxial Geogrid Reinforcement. International Journal of Advanced Engineering, Management and Science, 9, 8.

[7] Siva Chidambaram, R., & Agarwal, P. (2014). The confining effect of geo-grid on the mechanical properties of concrete specimens with steel fiber under compression and flexure. Construction and Building Materials, 71, 628–637.

[8] Siva Chidambaram, R., & Agarwal, P. (2015a). Flexural and shear behavior of geo-grid confined RC beams with steel fiber reinforced concrete. Construction and Building Materials, 78, 271–280.

[9] El-Kasaby, E. S. A., Awwad, M., Roshdy, M., & Abo-Shark, A. A. (2023). Behavior of Square footings reinforced with glass fiber bristles and biaxial geogrid. *European Journal of Engineering and Technology Research*, *8*(4), 5-11.

[10] Ali B, Qureshi LA. Influence of glass fibers on mechanical and durability performance of concrete with recycled aggregates. Constr Build Mater 2019;228: 116783. https://doi.org/10.1016/j.conbuildmat.2019.116783.

[11] Siva Chidambaram R, Agarwal P. The confining effect of geo-grid on the mechanical properties of concrete specimens with steel fiber under compression and flexure. Constr Build Mater 2014;71:628–37.

[12] Anandaraj S, Rooby J, Awoyera PO, Gobinath R. Structural distress in glass fibre-reinforced concrete under loading and exposure to aggressive environments. Constr Build Mater 2019;197:862–70.

[13] Ibrahim KIM. Mechanical properties of glass fiber reinforced concrete (GFRC). Journal of Mechanical and Civil Engineering. 2016;13(4).

[14] Shakor PN, Pimplikar SS. Glass fiber reinforced concrete use in construction. International Journal of Technology and Engineering System. 2011;2:2.

[15] Mohamed MA, Moh MA, Akasha NW, Elgady IYI. Experimental study on effects of fiberglass and fiber waste in concrete mixes. International Journal of Engineering Science & Research Technology. 2016;3:485-493.

[16] Graybeal A.B., Baby F. Development of Direct Tension Test Method for Ultra-High-Performance Fiber-Reinforced Concrete. ACI Materials Journal. 2013;110:177-186.

[17] Meng, X., Zhang, M., & Liu, S. (2019). Investigation of the mechanical properties of pervious concrete beams reinforced with biaxial geogrids. Construction and Building Materials, 198, 92-102. doi: 10.1016/j.conbuildmat.2018.11.118

[18] Susumu, I. (1994). Ductility and Energy Dissipation of Concrete Beam Members and Their Damage Evaluation Based on Hysteretic Dissipated Energy (Doctoral dissertation). Kyoto University, Kyoto, Japan.

[19] AACE International. Skills and Knowledge of Cost Engineering, 6th ed.; Hastak, M., Ed.; AACE International: Morgantown, WV, USA, 2015.